Redox Biology 81 (2025) 103576

Contents lists available at ScienceDirect

Redox Biology

journal homepage: www.elsevier.com/locate/redox

Succinate predisposes mice to atrial fibrillation by impairing mitochondrial function via SUCNR1/AMPK axis

Yudi Zhang [a,b,1], Haoyu Gong [a,1], Lingyan Jin [a], Peng Liu [a], Jiali Fan [a], Xinghua Qin [c,*], Qiangsun Zheng [a,**]

[a] Department of Cardiology, The Second Affiliated Hospital, Xi'an Jiaotong University (XJTU), China
[b] Department of Cardiology, Sir Run Run Shaw Hospital (SRRSH), Zhejiang University, China
[c] School of Life Sciences, Northwestern Polytechnical University, China

ARTICLE INFO

Keywords:
Atrial fibrillation
Succinate
Mitochondrial dysfunction
AMPK
Diabetes

ABSTRACT

Atrial fibrillation (AF), a major public health concern, is associated with high rates of death and disability. Mitochondrial dysfunction has emerged as a key contributor to the pathophysiology of AF. Succinate, an essential Krebs cycle metabolite, is often elevated in the circulation of patients at risk for AF. However, its exact role in AF pathogenesis is still not well understood. To explore the association linking succinate overload and AF, we first established AF-susceptible mouse models of obesity and diabetes, confirming that circulating succinate levels were significantly elevated in these AF-prone mice. Next, we assessed AF vulnerability and atrial remodeling in succinate-treated mice (2 %/5 % for 7 weeks) or isolated primary atrial cells (0.5 mM for 24 h). Our results demonstrated that succinate overload increased AF susceptibility in mice and triggered adverse atrial remodeling, characterized by left atrial dilation, connexins lateralization, ion channel disturbances, and fibrosis. Moreover, succinate compromised atrial mitochondrial structure, leading to increased oxidative stress. Mechanistically, succinate overload upregulated the expression of its cognate receptor SUCNR1 (succinate receptor 1) and decreased AMPK (AMP-activated protein kinase) phosphorylation both *in vitro* and *in vivo*. AICAR (AMPK activator) maintained mitochondrial health to mitigate remodeling in succinate-exposed cells and prevented succinate-induced AF in obese and diabetic mice. In conclusion, succinate overload enhances AF vulnerability and atrial remodeling by impairing AMPK signaling and mitochondrial function. Succinate, therefore, represents an underappreciated contributor to AF pathogenesis and a potential biomarker.

1. Introduction

Atrial fibrillation (AF) ranks as the commonest tachy-arrhythmia [1], and represents a major health concern due to its rising incidence and associated increase in both mortality and morbidity [2]. Despite ongoing advancements, diagnostic, preventive, and therapeutic options for AF remain limited. To develop more effective pharmacological and molecular therapies, it is crucial to identify the precise mechanisms underlying AF.

Metabolic disorders are critical triggers for AF [3,4]. Common metabolic disorders, such as obesity, diabetes, hypertension, and thyroid dysfunction, are major risk factors for AF [3]. Specifically, these metabolic abnormalities can disrupt atrial energy balance and substrate metabolism, triggering electrical instability and structural remodeling characterized by myocyte hypertrophy, fibroblast proliferation, and extracellular matrix alterations. Additionally, metabolic dysfunction promotes inflammation and oxidative stress, further exacerbating AF [5].

Mitochondria are pivotal to cardiac metabolism, serving as the heart's main energy producers. Approximately 95 % of the heart's energy is generated within mitochondria through the integration of the Krebs cycle, the electron transport chain (ETC), and oxidative phosphorylation (OXPHOS). As an energy-demanding organ, the heart relies on tightly regulated bioenergetics to align with nutrient availability and metabolic demands, ensuring atrial metabolic flexibility [6]. Mitochondrial dysfunction in the atria is widely recognized as a key

* Corresponding author.
** Corresponding author.
E-mail addresses: xinghuaqin@nwpu.edu.cn (X. Qin), zhengqs@mail.xjtu.edu.cn (Q. Zheng).
[1] Equally Contributed.

https://doi.org/10.1016/j.redox.2025.103576
Received 1 January 2025; Received in revised form 18 February 2025; Accepted 26 February 2025
Available online 26 February 2025
2213-2317/© 2025 The Authors. Published by Elsevier B.V. This is an open access article under the CC BY-NC-ND license (http://creativecommons.org/licenses/by-nc-nd/4.0/).

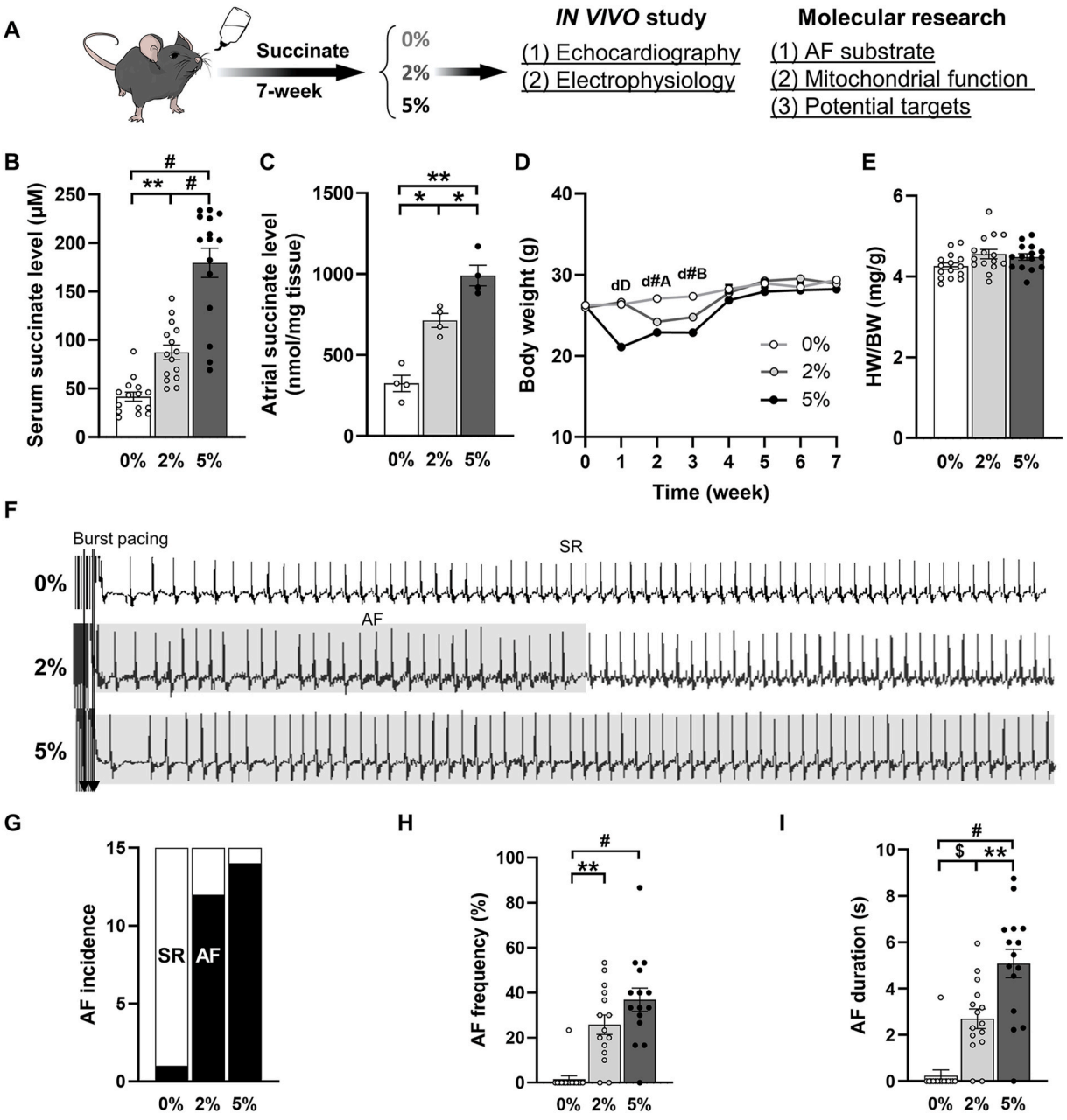

Fig. 1. Succinate overload increased AF susceptibility in mice. (A) Schematic representation of the animal experimental design. (B) Circulating and (C) atrial succinate concentrations in mice treated with 0 %, 2 % and 5 % (*w/v*) succinate in drinking water for 7 weeks. (D) Body weight (BW) and (E) heart weight-to-body weight ratio (HW/BW). (F) Representative trace of burst pacing-induced atrial fibrillation (AF) and the corresponding analysis of (G) AF incidence, (H) AF frequency, and (I) AF duration. SR, sinus rhythm; T2DM, type 2 diabetes. Data are shown as mean ± SEM. (A-B, D–I) n = 15; (C) n = 4. $^{*}p < 0.05$, $^{**}p < 0.01$, $^{\$}p < 0.001$, $^{\#}p < 0.0001$; (D) $^{\#}p < 0.0001$ 0 % vs. 2 %, $^{d}p < 0.0001$ 0 % vs. 5 %, $^{A}p < 0.05$ 2 % vs. 5 %, $^{B}p < 0.01$ 2 % vs. 5 %, $^{D}p < 0.0001$ 2 % vs. 5 %. (One-way ANOVA with Bonferroni *post-hoc* test).

mechanism linking metabolic derangements to AF pathogenesis, regardless of its underlying etiology [7]. This has led to increasing interest in targeting pivotal regulators of mitochondrial function and homeostasis as potential anti-AF therapeutic strategies, with AMP-activated protein kinase (AMPK) emerging as a particularly promising candidate [8,9]. Despite this progress, the precise mitochondrial mechanisms driving AF and the development of effective anti-AF therapies targeting mitochondrial dysfunction remain largely unexplored.

Succinate, an essential metabolite in the TCA cycle, is integral to mitochondrial bioenergetics and redox homeostasis [10] and has been highlighted as a potential AF risk factor. Physiologically, succinate occupies a central metabolic position, directly linking the mitochondrial TCA cycle to the ETC by donating electrons via flavin adenine dinucleotide (FAD) in mitochondrial complex II [11]. However, pathological succinate accumulation can disrupt mitochondrial function, leading to tissue damage and dysfunction through mechanisms such as reactive oxygen species (ROS) overproduction [12], abnormal epigenetic reprogramming [13], and post-translational modification [14]. Succinate can accumulate under various pathological conditions, including ischemia or hypoxia [15], and fibrillated hearts [16], and can also be released by dysbiosised gut flora [17], which is commonly observed in AF populations. Indeed, plasmatic succinate levels were elevated in patients with a history of AF risks encompassing obesity [18], hypertension, type 2 diabetes (T2DM) [19], cardiac ischemia [12], and other cardiovascular diseases [20]. Clinical evidence further reveals a direct

link between circulating succinate overloading and increased AF risk, stroke recurrence, and left atrial enlargement [21,22]. Experimental studies provide additional support for this association. Persistent AF induced by rapid pacing has been shown to elevate atrial succinate levels [16]. Moreover, succinate overload has been implicated in altering sinus node recovery time (SNRT) [16], promoting atrial fibrosis [23], and exacerbating inflammation and mitochondrial oxidative stress [24]. Together, these findings highlight succinate as a causative factor for AF with viable therapeutic potential.

Therefore, we propose that succinate is an underappreciated mitochondrial contributor to AF pathogenesis. However, the role of succinate in driving AF remains under-investigated. This study seeks to explore whether circulating succinate overload contributes to AF development and to elucidate the mechanistic link between succinate accumulation and AF pathogenesis, with a primary focus on mitochondrial dysfunction.

2. Materials and methods

2.1. Animal experiments

One hundred and five male C57BL/6J mice (5.5 ± 0.5 weeks, Xi'an Jiaotong University/XJTU, standard conditions) were used. Two AF-susceptible mice models were established to assess changes in circulating succinate concentrations under AF risk conditions. Diet-induced obesity (DIO) was induced by feeding mice a high-fat diet (#D12492; Research Diets, NJ, US) for 13 weeks, with obesity defined as a body weight (BW) 20 % heavier than the average of control mice. T2DM was established by a 4-week high-fat diet followed by streptozotocin injection (100 mg/kg; Sigma-Aldrich, St. Louis, US), and mice with fasting blood glucose >7.8 mmol/L were subsequently used for further experiments. Previous studies have reported elevated circulating succinate levels in mice with AF risk factors, including obesity, diabetes, hypertension, and nonalcoholic fatty liver disease, with doses of 2–5% (*w/v*) sodium succinate used in these studies [25,26]. In line with these findings, we exposed mice to a diet supplemented with 2 % and 5 % (*w/v*) sodium succinate in the present study. We further confirmed that the circulating succinate concentrations in obese or diabetic mice were comparable to those in mice receiving the succinate supplementation (Fig. 1B, Fig. S1D). Therefore, mice were administered water containing 0 %, 2 %, or 5 % (*w/v*) sodium succinate (V900102; Sigma-Aldrich) for 7 consecutive weeks. In addition, to activate AMPK *in vivo*, mice received a 200 mg/kg/day intraperitoneal injection of 5-aminoimidazole-4-carboxamide ribonucleotide (AICAR; TargetMol, Boston, US) for 2 weeks. All mice underwent electrophysiological and echocardiographic evaluation, followed by tissue sampling after sacrifice.

2.2. Cell experiments

Newborn Sprague-Dawley rat atria were dissected and digested using Type II collagenase (0.1 %; Solarbio, Beijing, China) to isolate primary atrial cells. The dispersed cells were seeded into culture plates and separated by a 2-h differential attachment. Neonatal rat cardiac fibroblasts (NRCFs) were identified using anti-vimentin immunofluorescence (>90 % purity), and neonatal rat cardiomyocytes (NRCMs) were identified under a light microscope.

Isolated cells were cultured in DMEM supplemented with FBS (10 %; Invitrogen, Carlsbad, US) in a humidified incubator with 5 % CO_2 at 37 °C. NRCFs from the 2nd-4th passage and confluent NRCMs were used for the experiments. Cells were transfected with siRNA (Table S1; Sangon, Shanghai, China) using the lipofectamine 3000 (Invitrogen) for 48 h to genetically suppress succinate receptor 1 (SUNCR1), or incubated with AICAR (0.5 mM) for 24 h to activate AMPK. To determine the appropriate concentration of succinate in cellular experiments, we treated NRCFs with the increasing concentration of sodium succinate (0, 50, 500, 1000, 2000, and 5000 μM) [25], and found that 0.5 mM sodium succinate significantly enhanced NRCFs' proliferation and increased their protein levels of fibrosis markers (Fig. S2). Cells were then exposed to succinate (0.5 mM, 24 h) before harvesting.

2.3. Electrophysiological study

Electrodes catheters were inserted into the esophagus at the atrial level, and *trans*-esophageal atrial pacing was performed using a VCS3001 stimulator (MappingLab, Oxford, UK). Surface electrocardiograms were recorded using an RM6240E system (Chengdu Instrument Factory, Chengdu, China), and baseline electrophysiological parameters were averaged over 10 cardiac cycles. Burst pacing (5 s, 1.5 × threshold current, pulse width 1 ms) was applied at frequencies of 30, 35, and 40 Hz (10 times each) to assess AF inducibility, with AF defined as an irregular, rapid atrial rhythm lasting > 1s. Atrial effective refractory period (ERP) was measured using an S1S2 pacing protocol. Maximum sinoatrial node recovery time (SNRTmax) was measured using a 10-s pacing protocol (basic cycle length: 140 ms). The corrected SNRTmax ($CSNRT_{max}$) was calculated as [$SNRT_{max}$ - R–R interval].

2.4. Echocardiographic evaluation

A Vevo 2100 scanner (VisualSonics, Toronto, Canada) was utilized to perform the echocardiographic examination on isoflurane-anesthetized mice. Left atrial (LA) filling volume was estimated using the formula: π/6·[anteroposterior dimension (AP) · superoinferior dimension (SI) · mediolateral dimension (ML)], as described previously [27]. Results were averaged over 3 cardiac cycles.

2.5. Histology study

Paraffin-embedded atrial slides (5 μm) were stained with Masson's trichrome, hematoxylin (H) & eosin (E), WGA (Wheat Germ Agglutinin), or immunohistochemistry. Stained sections were imaged using a digital slice scanner (WINMEDIC, Jinan, China). Six random fields from each slide were analyzed in a blinded manner using Fiji image analysis software (NIH, Bethesda, USA).

2.6. Transmission electron microscopy (TEM)

Ultrathin sections (60 nm) stained with uranyl acetate (2 %) - lead citrate (2.6 %) were photographed by TEM (H-800, 80 kV; Hitachi, Tokyo, Japan). Mitochondrial morphology was analyzed by stereology using the point-counting method in Fiji software. A total of 60 mitochondria from five randomly selected cells were evaluated.

2.7. Mitochondrial DNA (mtDNA) and mitochondrial protein (mtProtein) quantification

Atrial mitochondria were isolated (Beyotime, Shanghai, China). The mtProtein levels were measured using a bicinchoninic acid (BCA) protein assay (Pierce, Rockford, US) and normalized to the total protein content. Relative mtDNA content was quantified using real-time quantitative polymerase chain reactions (RT-qPCR). The ratio of mtDNA (target gene: *Nd1*) to nuclear DNA (target gene: *HK2*) was used to determine relative mtDNA content.

2.8. Mitochondrial respiratory enzymatic activities assay and succinate evaluation

Mitochondrial ATP content was quantified using a commercial ATP assay kit (BC0305; Solarbio). Mitochondrial respiratory chain complexes, including I, II, and III, and succinate concentrations were determined using specific commercial assay kits (CSB-EQ027280MO, CUSABIO; BC3235 and BC3245, Solarbio; #K-SUCC, MEGAZYME, Wicklow, Ireland).

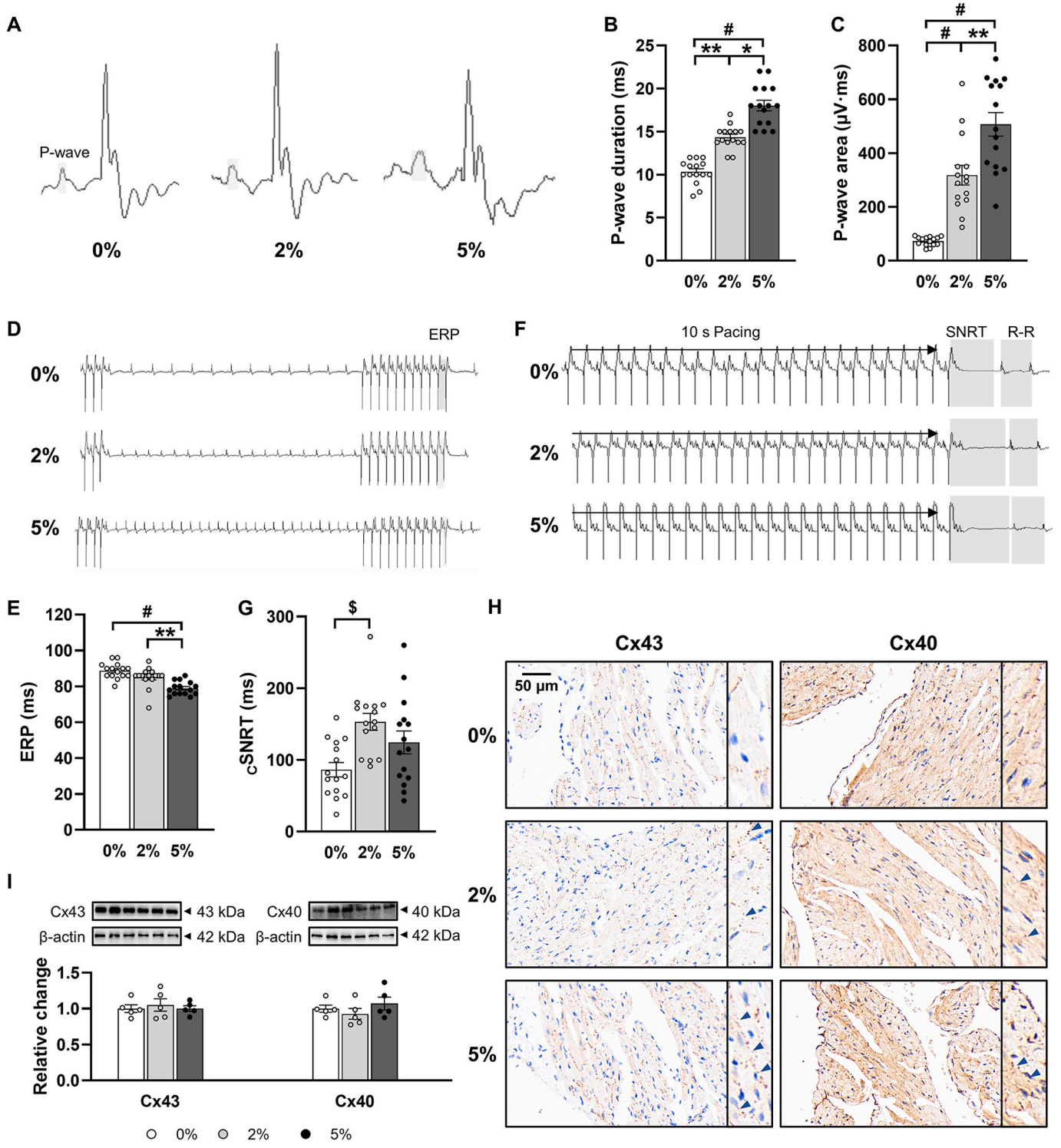

Fig. 2. Succinate overload induced electrical remodeling in mice. (A) Representative P-wave traces, (B) P-wave duration, and (C) P-wave area in mice treated with 0 %, 2 %, or 5 % (*w/v*) succinate. (D) Representative traces and (E) corresponding analysis of the effective refractory period (ERP). (F) Representative traces and (G) corresponding analysis of the maximum corrected sinus node recovery time ($CSNRT_{max}$). (H) Immunohistochemical staining and (I) Western blot analysis of atrial Cx43 and Cx40 expression. Triangles indicate lateralization of connexins. Cx, connexin-. Data are shown as mean ± SEM. (A–G) n = 15; (H–I) n = 4–5. $^{*}p < 0.05$, $^{**}p < 0.01$, $^{\$}p < 0.001$, $^{\#}p < 0.0001$ (One-way ANOVA with Bonferroni *post-hoc* test). (H) Scale bar = 50 μm.

2.9. Oxidative stress assay

The mitochondrial superoxide indicator MitoSOX was used to quantify the mitochondrial superoxide in freshly frozen atrial sections (5 mM, 20 min; Molecular Probes, Eugene, OR, US). Dihydroethidium (DHE) was applied to label intracellular superoxide in atrial tissue (5 μM; 30 min; Molecular Probes) or cells (1 mM, 30 min). Sections were immediately photographed by a fluorescence microscope (Nikon, Melville, NY, US). The oxidative stress, indicated by the red fluorescence signal, was quantified using Fiji software. Malondialdehyde and superoxide dismutase (SOD) activity were evaluated following the manufacturer's protocols (Beyotime).

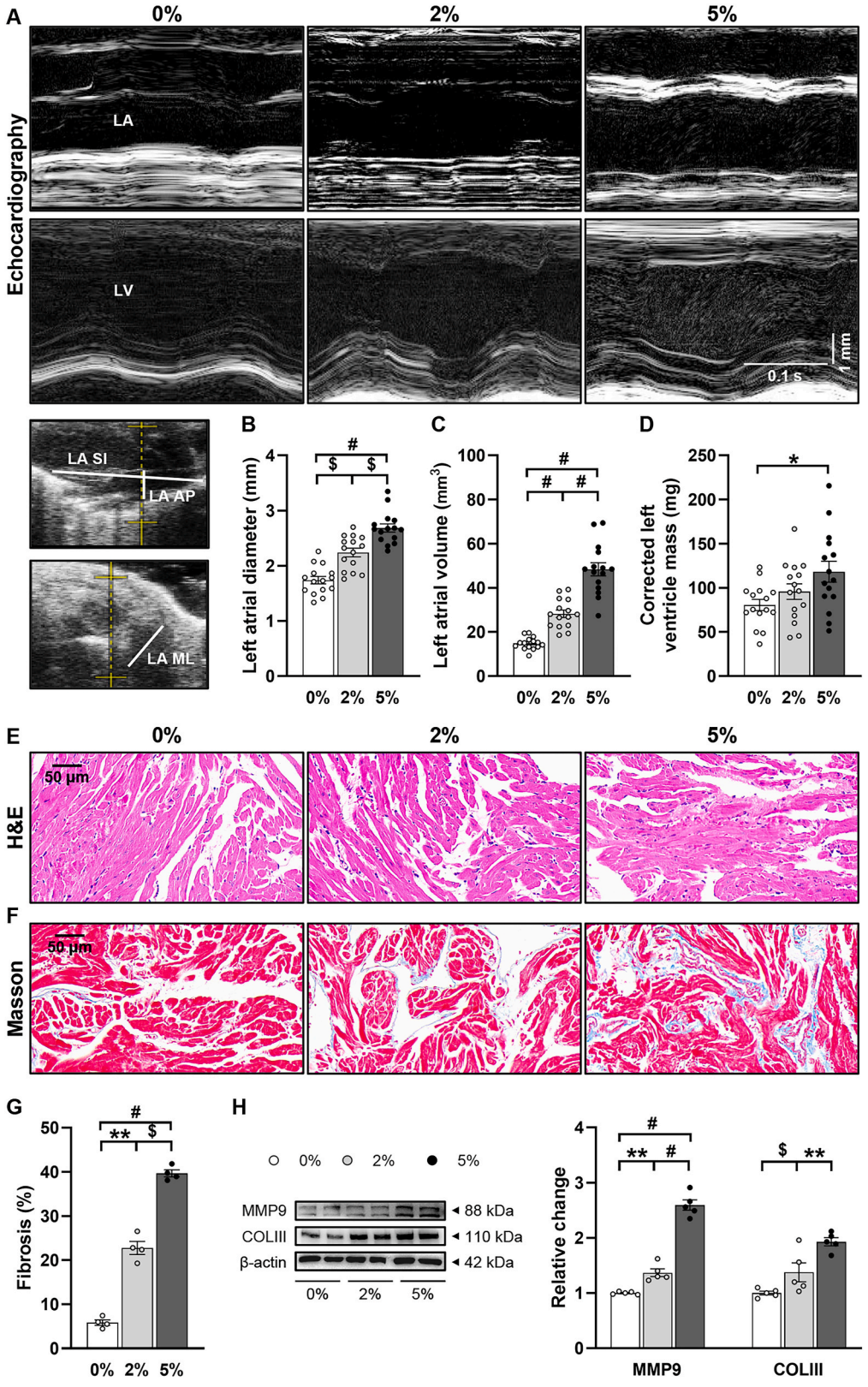

Fig. 3. *Succinate overload altered atrial structure in mice.* (A) M-mode echocardiographic images of left atria (LA) and left ventricle (LV) and corresponding analysis of (B) left atrial diameter, (C) left atrial volume, and (D) corrected ventricle mass in mice treated with 0 %, 2 %, or 5 % (*w/v*) succinate. (E) Representative hematoxylin-eosin (H&E) staining images of atrial tissue among groups. (F) Representative Masson' trichrome staining images and (G) quantification of atrial fibrosis among groups. (H) Representative Western blot images and quantification of fibrosis markers, including matrix metallopeptidase 9 (MMP9) and collagen III (COLIII) in atrial tissue. AP, anteroposterior dimension; MI, mediolateral dimension; SI, superoinferior dimension. Data are shown as mean ± SEM. (B–D) n = 15; (E–H) n = 4–5. $^{*}p < 0.05$, $^{**}p < 0.01$, $^{\$}p < 0.001$, $^{\#}p < 0.0001$ (One-way ANOVA with Bonferroni *post-hoc* test). (E–F) Scale bar = 50 μm.

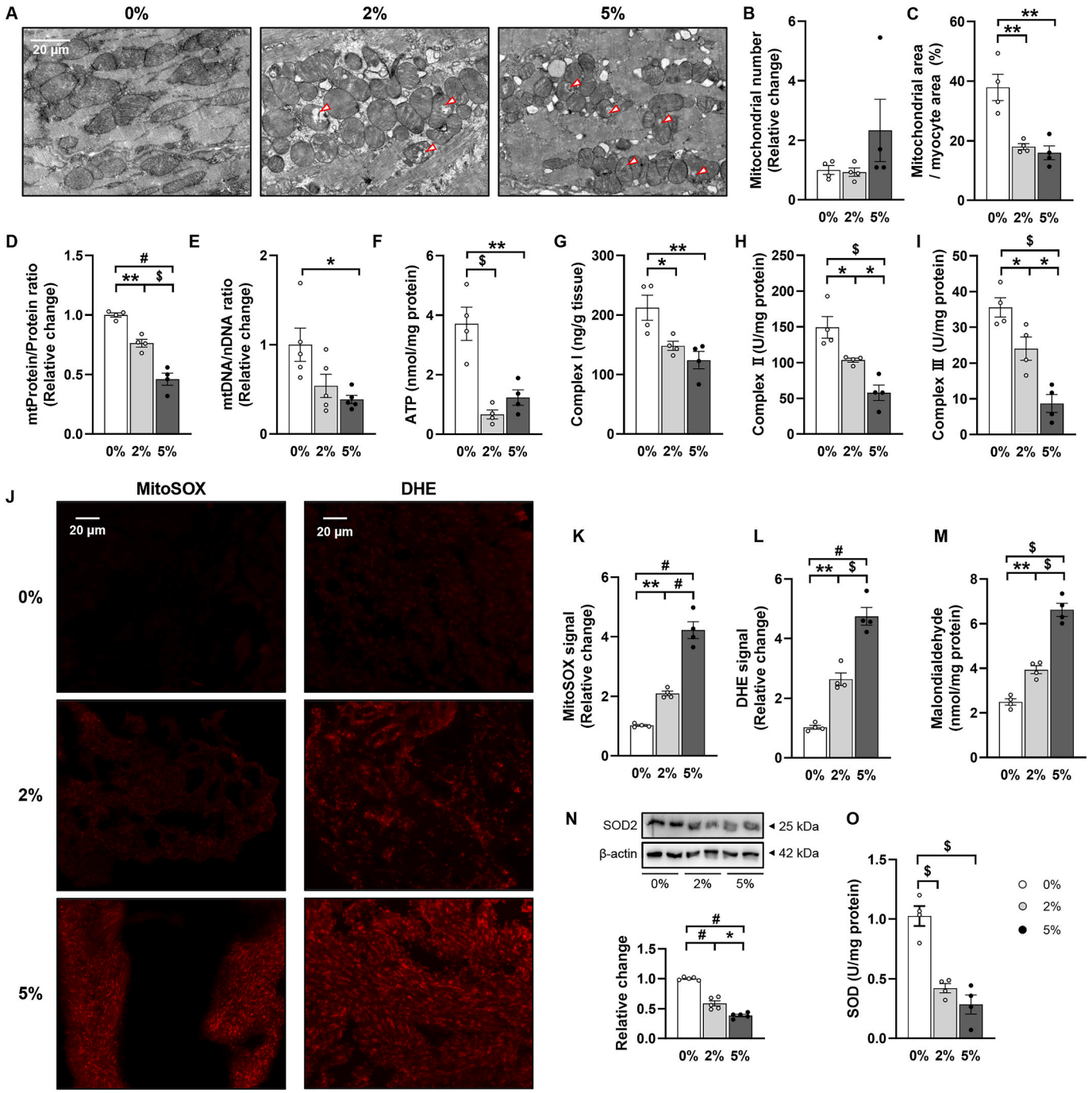

Fig. 4. Succinate overload impaired mitochondrial function in the atria **of mice.** (A) Representative longitudinal transmission electron microscope (TEM) images showing mitochondrial morphology in the atria and quantification of (B) mitochondrial number and (C) mitochondrial volume density. Triangles indicate the mitochondrial swelling. (D) Quantification of atrial mitochondrial protein (mtProtein) and (E) mitochondrial DNA (mtDNA) content. (F) Measurement of atrial ATP content and the enzymatic activity of mitochondrial complexes: (G) complex I, (H) complex II, and (I) complex III. (J) Representative images and quantification of atrial oxidation products labeled by (K) MitoSOX and (L) dihydroethidium (DHE). (M) Quantification of atrial malondialdehyde (MDA) levels. (N) Representative Western blot images and quantification of superoxide dismutase 2 (SOD2) protein expression in the atria. (O) Measurement of atrial SOD activity. Data are shown as mean ± SEM. n = 4. $^{*}p < 0.05$, $^{**}p < 0.01$, $^{\$}p < 0.001$, $^{\#}p < 0.0001$ (One-way ANOVA with Bonferroni *post-hoc* test). (A, J) Scale bar = 20 μm.

2.10. Mitochondrial membrane potential (Δψm) assay

Cells were treated with JC-1 dye (2 μM; Invitrogen, 37 °C, 30 min) to assess Δψm. Fluorescence images were immediately acquired (Nikon). In each independent experiment, 20 cells were analyzed using Fiji software. A reduction in the red/green fluorescence ratio indicated a loss or collapse of Δψm.

2.11. Cell viability assay

Cells were plated (1×10^4 cells/each 96-well) and exposed to the indicated drugs for 24 h. Following treatment, cell viability was then assessed by the Cell Counting Kit-8 (CCK-8, Sigma-Aldrich) method. After incubation with CCK-8 (10 % v/v, 37 °C, 1.5–2 h), cell absorbance at 450 nm was determined using a microplate reader. Each experiment was performed in 6 replicates.

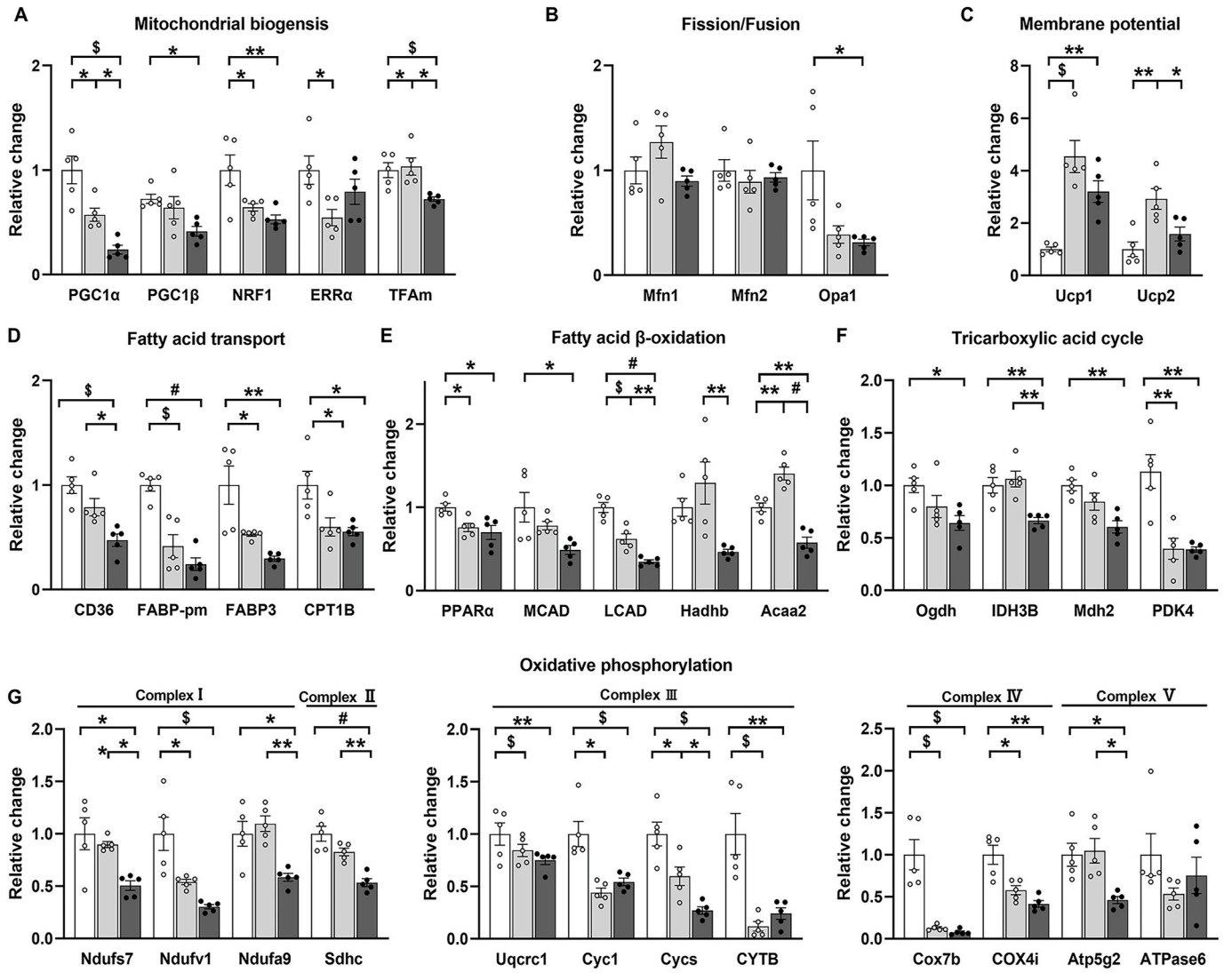

Fig. 5. Succinate overload induced a shift in the transcriptional profile of mitochondrial health-related genes in the atri*a of mice.* RT-qPCR assays of mitochondrial health-related genes involved in (A) mitochondrial biogenesis, (B) mitochondrial fusion/fission, (C) mitochondrial membrane potential, (D) fatty acid transport, (E) fatty acid β-oxidation, (F) the tricarboxylic acid (TCA) cycle, and (G) oxidative phosphorylation. Data are shown as mean ± SEM. n = 5. $^{*}p < 0.05$, $^{**}p < 0.01$, $^{\$}p < 0.001$, $^{\#}p < 0.0001$ (One-way ANOVA with Bonferroni *post-hoc* test).

2.12. Cell migration analysis

To measure cell migration, a scratch was made in serum-starved NRCFs (90–100 % confluence) by sterile 10 μL pipette tips. The cells were subsequently washed twice to clean cellular debris and stimulated with the indicated drugs. Photomicrographs were captured (Leica) at 0, 6, and 24 h post-scratch. The percentage of wound closure area was analyzed from 5 independent experiments using Fiji software to assess cell migration.

2.13. RT-qPCR

Total RNA was extracted using TRIzol (Invitrogen). cDNA was subsequently synthesized from the extracted RNA using a reverse transcription kit (Accurate Biology, Changsha, China). Gene expression was quantified by RT-qPCR using SYBR Green (Accurate Biology) on a CFX96 Real-Time PCR Detection System (Bio-Rad, CA, US). Primer sequences are listed in Table S2. Relative gene expression levels were normalized to β-actin using the $2^{-\Delta\Delta Ct}$ method.

2.14. Western blot (WB)

Extracted protein was separated by SDS-PAGE (10–12 %), transferred to PVDF membranes, and blocked with 5 % non-fat milk. The membranes were incubated with primary antibodies (Table S2) at 4 °C overnight, followed by incubation with secondary antibodies at room temperature for 2 h. Immunoreactive bands were detected by chemiluminescence (Tanon, Shanghai, China) and quantified using Quantity One software (Bio-Rad).

2.15. Statistics

Statistical analyses were conducted using SPSS (IBM, NY, US). Data are presented as mean ± SEM. One-/two-way analysis of variance (ANOVA) was employed to compare means between groups, followed by Bonferroni *post-hoc* tests to identify specific differences. $p < 0.05$ was considered significant.

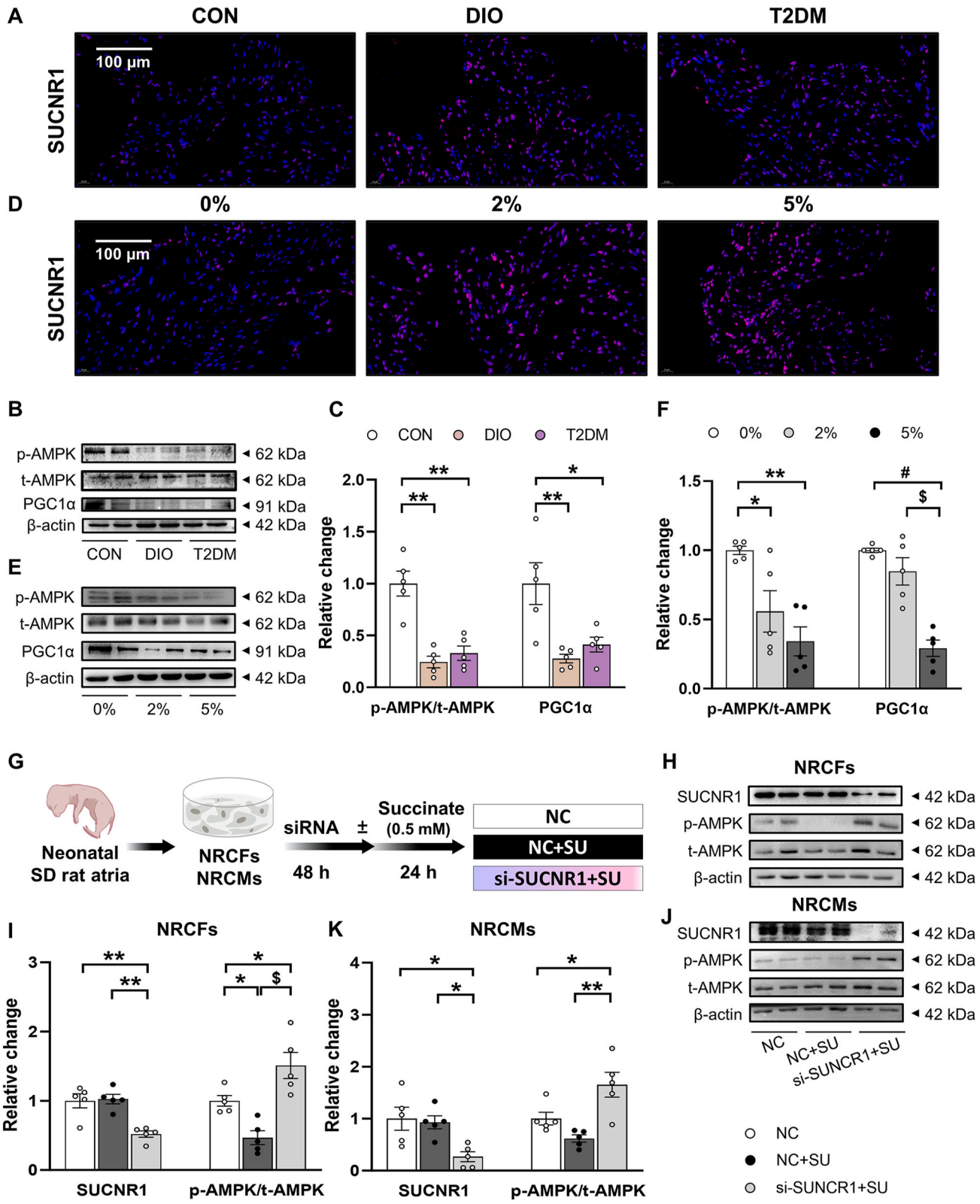

Fig. 6. The SUCNR1/AMPK axis mediated succinate-*induced AF.* (A) Immunohistochemical analysis of atrial succinate receptor 1 (SUCNR1) expression and (B–C) Western blot analysis of atrial AMPK/PGC1α signaling in control (CON), diet-induced obesity (DIO), type 2 diabetes (T2DM) mice. (D) Immunohistochemical analysis of atrial SUCNR1 expression and (E–F) Western blot analysis of atrial AMPK/PGC1α signaling in mice treated with 0 %, 2 %, or 5 % (*w/v*) succinate. Red: SUCNR1; Blue: DAPI. (G) Schematic representation of the cell experimental design. (H) Representative Western blot images and (I) quantification of SUCNR1 and AMPK signaling in isolated neonatal rat cardiac fibroblasts (NRCFs). (G) Schematic representation of the cell experimental design. (J) Representative Western blot images and (K) quantification of SUCNR1 and AMPK signaling in isolated neonatal rat cardiomyocytes (NRCMs). NC, negative control; PGC1α, peroxisome proliferator-activated receptor-γ coactivator; p-/t-AMPK, phosphorylated/total adenosine monophosphate-activated protein kinase; SU, succinate. Data are shown as mean ± SEM. n = 4–5. $^{*}p < 0.05$, $^{**}p < 0.01$, $^{\$}p < 0.001$, $^{\#}p < 0.0001$ (One-way ANOVA with Bonferroni *post-hoc* test). (A–B) Scale bar = 100 μm.

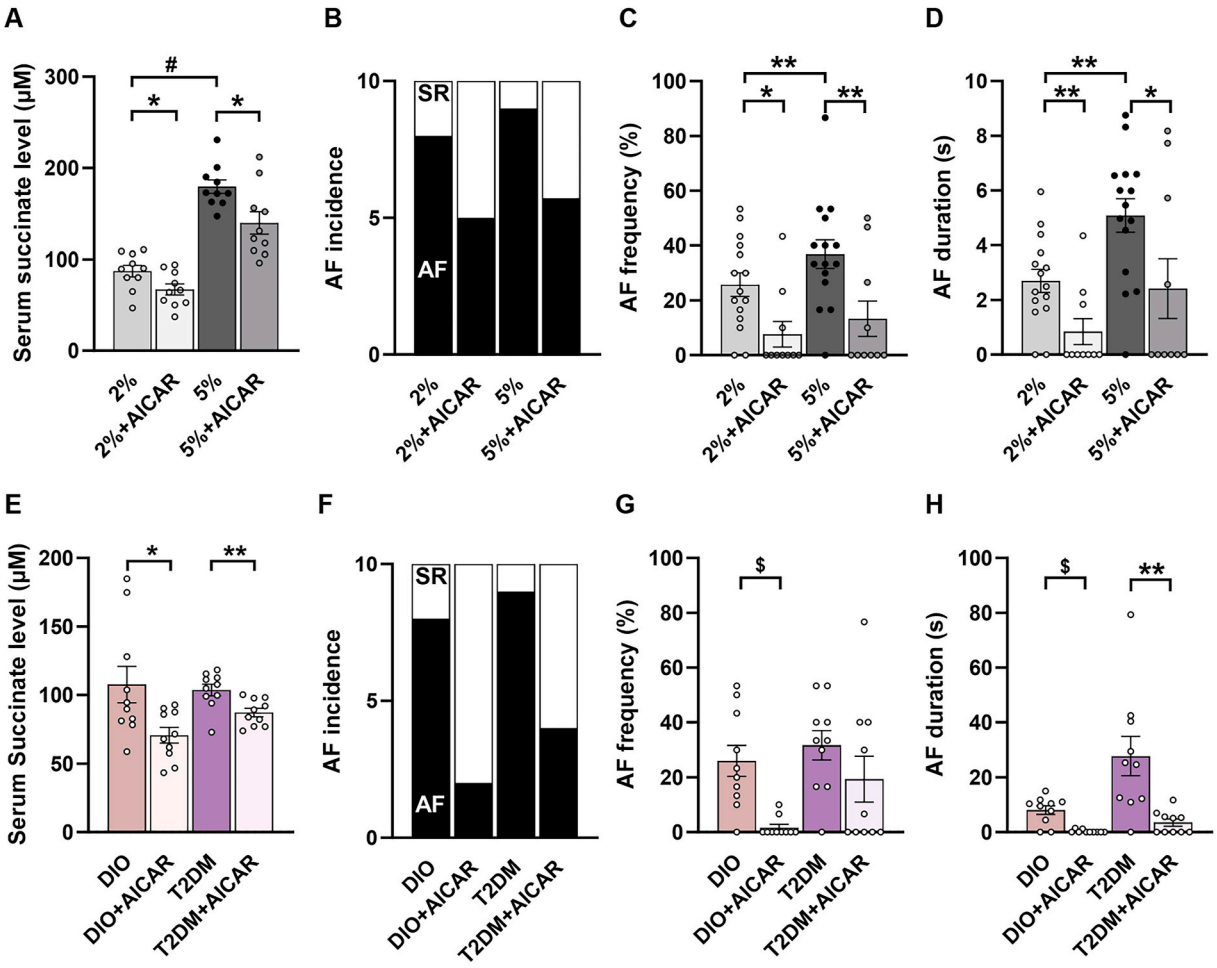

Fig. 7. AMPK activation via AICAR *mitigated DIO, T2DM, or succinate-induced AF in mice.* (A) Serum succinate levels, (B) atrial fibrillation (AF) incidence, (C) AF frequency, and (D) AF duration in succinate-induced AF-susceptible mice with or without two weeks of 5-aminoimidazole-4-carboxamide ribonucleotide (AICAR) treatment. (E) Serum succinate levels, (F) AF incidence, (G) AF frequency, and (H) AF duration in diet-induced obesity (DIO) and type 2 diabetes (T2DM) mice with or without two weeks of AICAR treatment. Data are shown as mean ± SEM. n = 10–15. $^{*}p < 0.05$, $^{**}p < 0.01$, $^{\$}p < 0.001$, $^{\#}p < 0.0001$ (Two-way ANOVA with Bonferroni *post-hoc* test).

3. Results

3.1. Elevated circulating succinate levels in AF-susceptible mice

To identify the causal relationship between succinic acid and AF development, we initially compared the circulating succinate concentration in healthy control mice and mice with well-established AF risk factors, including T2DM and obesity. The circulating succinate levels increased in both DIO and T2DM mice, which are prone to developing AF (Fig. S1).

To clarify whether succinate overload mediates AF pathogenesis, we supplemented mice with 0 %, 2 %, or 5 % *w/v* sodium succinate for 7 weeks (Fig. 1A). Water consumption data indicated no aversion to succinate-containing water (Table S3). Mice exposed to 2 %/5 % (*w/v*) sodium succinate exhibited serum succinate overload comparable to that observed in DIO and T2DM mice, accompanied by atrial succinate accumulation (Fig. 1B and C). In addition, BW decreased during the first 4 weeks of succinate supplementation but showed no significant difference by the end of the experiment (Fig. 1D). Heart weight (HW) and the HW/BW ratio were unaffected by succinate treatment (Fig. 1E).

Importantly, succinate overload significantly predisposed mice to AF (Fig. 1F–I). Mice treated with sodium succinate displayed markedly increased AF inducibility (Fig. 1G), AF frequency (Fig. 1H), and AF duration (Fig. 1I), with these effects intensifying in a dose-dependent manner.

3.2. Succinate-induced atrial remodeling in mice

To further investigate how succinate enhances AF inducibility, we evaluated the atrial remodeling in mice, focusing on both electrical and structural changes. Succinate induced a series of electrophysiological changes associated with AF, including prolonged P-wave duration (Fig. 2A and B), increased P-wave area (Fig. 2C), and shortened ERP (Fig. 2D and E). Notably, 2 % (*w/v*) succinate significantly prolonged $CSNRT_{max}$ compared to the control, whereas the higher dose increased the dispersion of $CSNRT_{max}$ without reaching statistical significance (Fig. 2F and G). Additionally, histological staining demonstrated succinate-induced lateralization of connexin-40 (Cx40) and connexin-43 (Cx43), without affecting their overall atrial protein levels (Fig. 2H and I).

To assess the impact of succinate on atrial structure and function, we performed echocardiography, histological staining, and WB. Echocardiographic analysis showed that succinate increased LA diameter and LA filling volume, indicating LA dilation (Fig. 3A–C). Cardiac function remained unaltered after succinate overloading (Table S3). Histological and molecular analyses revealed a marked increase in atrial collagen content and expression of fibrosis markers, such as matrix metalloproteinase 9 (MMP9) and collagen III (Fig. 3E–H).

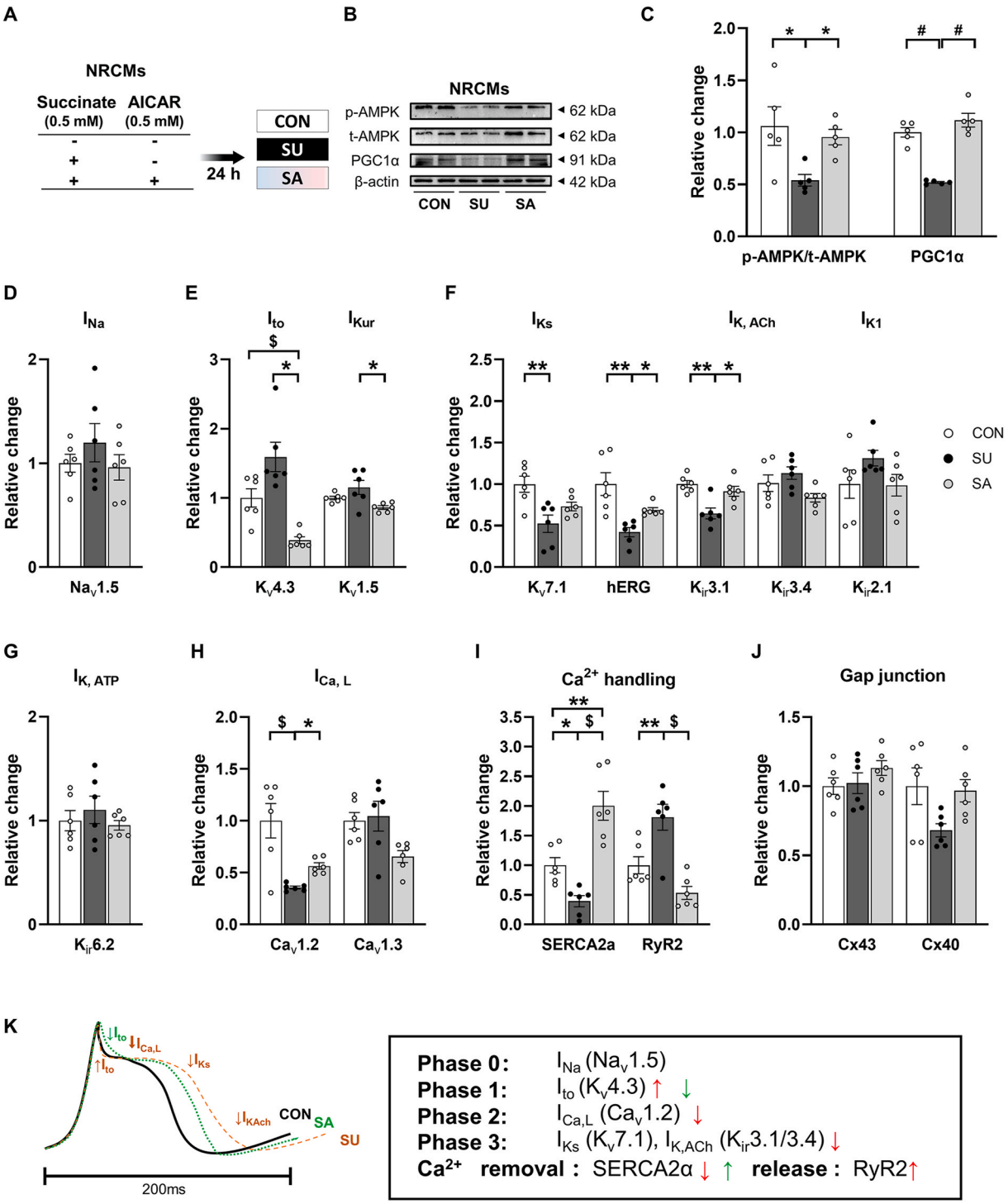

Fig. 8. AMPK activation via AICAR *alleviated succinate-induced electrical remodeling in NRCMs.* (A) Schematic representation of the cell experimental design. (B) Representative Western blot images and (C) quantification of AMPK and PGC1α signaling in isolated NRCMs treated with succinate and/or AICAR. RT-qPCR analysis of (D) sodium channel gene ($N_{av}1.5$), (E–G) potassium channel genes ($K_v4.3$, $K_v1.5$, $K_v7.1$, hERG, $K_{ir}3.1$, $K_{ir}3.4$, $K_{ir}2.1$, $K_{ir}6.2$), (H–J) calcium channel genes ($C_{av}1.2$, $C_{av}1.3$, SERCA2a, RYR2), and gap junction genes (Cx43, Cx40) in NRCMs treated with succinate and/or AICAR. (K) The typical shape of an atrial action potential (AP) and its potential morphological changes based on ion channel transcription levels. Cx, connexin-. Data are presented as mean ± SEM. n = 5–6. $^{*}p < 0.05$, $^{**}p < 0.01$, $^{\$}p < 0.001$, $^{\#}p < 0.0001$ (One-way ANOVA with Bonferroni *post-hoc* test).

3.3. *Succinate impaired atrial mitochondrial function in mice*

As succinic acid is an essential TCA cycle intermediate, we hypothesized that excessive succinate could disrupt mitochondrial function and contribute to AF. To test this hypothesis, we examined mitochondrial morphology and function in the atria of succinate-treated mice. TEM revealed that succinate reduced mitochondrial cristae surface density and mitochondrial volume density in the atria (Fig. 4A–C). Additionally, succinate significantly decreased mtDNA content and mitochondrial protein levels (Fig. 4D and E). Furthermore, succinate reduced ATP production, likely due to impaired activity of mitochondrial complexes I-III (Fig. 4F–I).

Redox imbalance is a key factor in mitochondrial dysfunction and AF pathogenesis. Consistent with this, increased levels of both cellular and mitochondrial ROS were observed, as determined by DHE and MitoSOX, respectively (Fig. 4J–L). Additionally, succinate treatment increased malondialdehyde levels and decreased superoxide dismutase 2 (SOD2) expression and activity, indicating a weakened antioxidant defense system (Fig. 4M–O).

To further investigate the mechanisms underlying succinate-associated mitochondrial dysfunction, we determined related gene levels. Succinate induced a coordinated down-regulated gene expression involved in mitochondrial biogenesis (*PGC1α*, *PGC1β*, *NRF1*, *ERRα*, *TFAM*), fusion/fission (*Opa1*), fatty acid transportation (*CD36*, *FABP-pm*, *FABP3*, *CPT1B*), fatty acid β oxidation (*PPARα*, *MCAD*, *LCAD*, *Hadhb*, *Acaa2*), the TCA cycle (*Ogdh*, *IDH3B*, *Mdh2*, *PDK4*), and oxidative phosphorylation (*Ndufs7*, *Ndufv1*, *Ndufa9*, *Sdhc*, *Uqcrc1*, *Cyc1*, *Cycs*, *CYTB*, *Cox7b*, *Cox4i*, *Atp5g2*) (Fig. 5A–G). Additionally, succinate upregulated the expression of genes regulating *Δψm*, like *UCP1* and *UCP2* (Fig. 5C).

3.4. SUCNR1/AMPK axis contributed to succinate-induced AF

As noted above, succinate impaired atrial metabolic capacity, prompting further investigation into AMPK signaling, a critical regulator of cellular metabolism and mitochondrial function. We observed an upregulated atrial expression of its receptor (SUCNR1) in AF-susceptible DIO, T2DM, and succinate-treated mice, accompanied by notable inhibition of AMPK signaling (Fig. 6A–F). Furthermore, PGC1α, a key downstream target of AMPK, was also downregulated in these mice (Fig. 6B, C, E, F), corroborating previous transcriptional findings (Fig. 5A).

To directly investigate the link between succinate/SUCNR1 and AMPK, we employed siRNA to genetically suppress SUCNR1 (Fig. 6J). siRNA-mediated suppression of SUCNR1 expression attenuated succinate-induced AMPK inactivation in both NRCFs (Fig. 6H and I) and NRCMs (Fig. 6J and K), suggesting that AMPK inactivation may underlie the pro-arrhythmic effects of succinate.

3.5. AMPK activation via AICAR mitigated succinate-induced AF and associated pathologies by improving mitochondrial function

To identify the precise role of AMPK activation in succinate-induced AF, we activate AMPK using AICAR. Two weeks of intraperitoneal AICAR administration (200 mg/kg) significantly reduced circulating succinate levels in succinate-supplemented mice (Fig. 7A). AICAR treatment also notably attenuated AF incidence, frequency, and duration in these mice (Fig. 7B–D). Similarly, AICAR reduced plasma succinate levels in DIO and T2DM mouse models, concurrently lowering their susceptibility to AF (Fig. 7E–H). These results suggest that AMPK activation can effectively reverse AF susceptibility in mice subjected to succinate overload, whether due to direct supplementation or metabolic disorders such as DIO and T2DM.

Given the lack of overt hypertrophy (Fig. S3), we explored whether succinate induced underlying microscopic alterations, such as ion channel remodeling. NRCMs were treated with succinate (0.5 mM) alone or in combination with AICAR (0.5 mM) for 1 day, and WB analysis confirmed the activation of AMPK/PGC1α signaling by AICAR (Fig. 8B and C). Succinate did not significantly affect the transcription of the sodium channel $N_{av}1.5$ (Fig. 8D). However, it downregulated the transcription of genes encoding potassium currents involved in phase 4 repolarization ($K_v7.1$, hERG, $K_{ir}3.1$), an effect reversed by AICAR treatment (Fig. 8E–G). Additionally, succinate decreased the transcription of genes that removes intracellular calcium (SERCA2a, $C_{av}1.2$), while upregulating the transcript of RYR2, a calcium-leaking channel (Fig. 8H and I). Notably, AICAR reversed these transcriptional abnormalities in calcium cycling regulators (Fig. 8H and I). Succinate, however, had no significant impact on the transcription of connexins such as Cx43 and Cx40 (Fig. 8J). In summary, succinate induced significant changes in the transcriptional profile of ion channels, potentially impairing cardiomyocyte function, and these adverse effects were effectively mitigated by AICAR treatment (Fig. 8K).

To determine whether the pro-fibrotic effects of succinate were directly mediated by its action on NRCFs or were secondary to dysfunction in NRCMs, and to evaluate whether AICAR could reverse these effects, we examined the impact of AICAR (0.5 mM, 24 h) on NRCFs treated with succinate (Fig. 8A). WB analysis confirmed that AICAR restored succinate-inhibited AMPK signaling and upregulated the expression of its downstream target, PGC1α (Fig. 8B and C). AICAR significantly suppressed the migration rate of NRCFs (Fig. 8D and E), reduced cell viability (Fig. 8F), and downregulated fibrosis markers' expression (MMP9, collagen I, collagen III) (Fig. 8G and H). These findings indicate that AMPK activation mitigates succinate-induced atrial fibrosis, providing a potential mechanism for the reduced AF susceptibility observed *in vivo*.

Finally, we examined whether AICAR protection against succinate-induced AF is mediated by its actions on mitochondrial function. AICAR treatment preserved mitochondrial structure (Fig. 10A–C), alleviated oxidative stress (Fig. 10D and E), and recovered mitochondrial membrane potential (Δψm) in NRCFs treated with succinate (Fig. 10F and G). Similar results were observed in NRCMs (Fig. 10H–N). These findings provide compelling evidence that AMPK activation via AICAR combats succinate-induced AF by preserving mitochondrial health and function.

4. Discussion

Our findings provide the first direct evidence of a dose-dependent relationship between succinate levels and AF risk. Further exploration revealed that succinate overload induces significant atrial remodeling, encompassing both electrical remodeling (ion channel and gap junction remodeling) and structural remodeling (left atrial dilation and fibrosis). Mechanistically, these effects were attributed to succinate-induced atrial mitochondrial dysfunction mediated by impaired SUCNR1/AMPK signaling. This study not only highlights a mitochondrial mechanism underlying AF pathogenesis but also suggests succinic acid as a potential novel AF marker and treatment objective, particularly under metabolic conditions such as obesity and diabetes.

Our findings emphasize succinate overload as a novel mitochondrial mechanism driving AF. Mitochondria are multifunctional: Beyond energy production, they play essential roles in regulating metabolic balance, apoptosis, cell proliferation, differentiation, redox state, and intracellular Ca^{2+} handling. By modulating signaling pathways, releasing mtDNA, interacting with organelles, and supplying metabolites, mitochondria are vital for maintaining normal cardiac function and structure. Clinical data has reported alterations in mitochondrial transcription profiles, protein expression, and metabolites in the atria of patients with AF [3]. Experimental studies further highlighted three key mitochondrial mechanisms underlying AF pathogenesis: energy deficiency [3,28], redox imbalance [29], and Ca^{2+} overload [30]. Succinate accumulation, a well-recognized marker of mitochondrial disturbance, has been shown to exacerbate these processes. Specifically, succinate induces pseudohypoxia under normoxic conditions by inhibiting prolyl-hydroxylases (PHDs)-induced hypoxia-inducible factor (HIF)-1α hydroxylation [31] and shifts metabolism from fat oxidation to glycolysis [15], impairing ketone body and lipid utilization. Additionally, succinate suppresses mitochondrial respiration through epigenetic [13] and post-translational modifications [14], and generates excessive ROS at mitochondrial complex I via reverse electron transport [32] and succinate dehydrogenase (SDH) oxidation [25]. Beyond regulating mitochondrial energetics, succinate overload disrupts mitochondrial quality control [33], alters mitochondrial permeability transition [34], impairs bioenergetics [35] and metabolic flux [31], and disturbs Ca^{2+} handling [36] and redox homeostasis in atrial tissue (Fig. 4). These

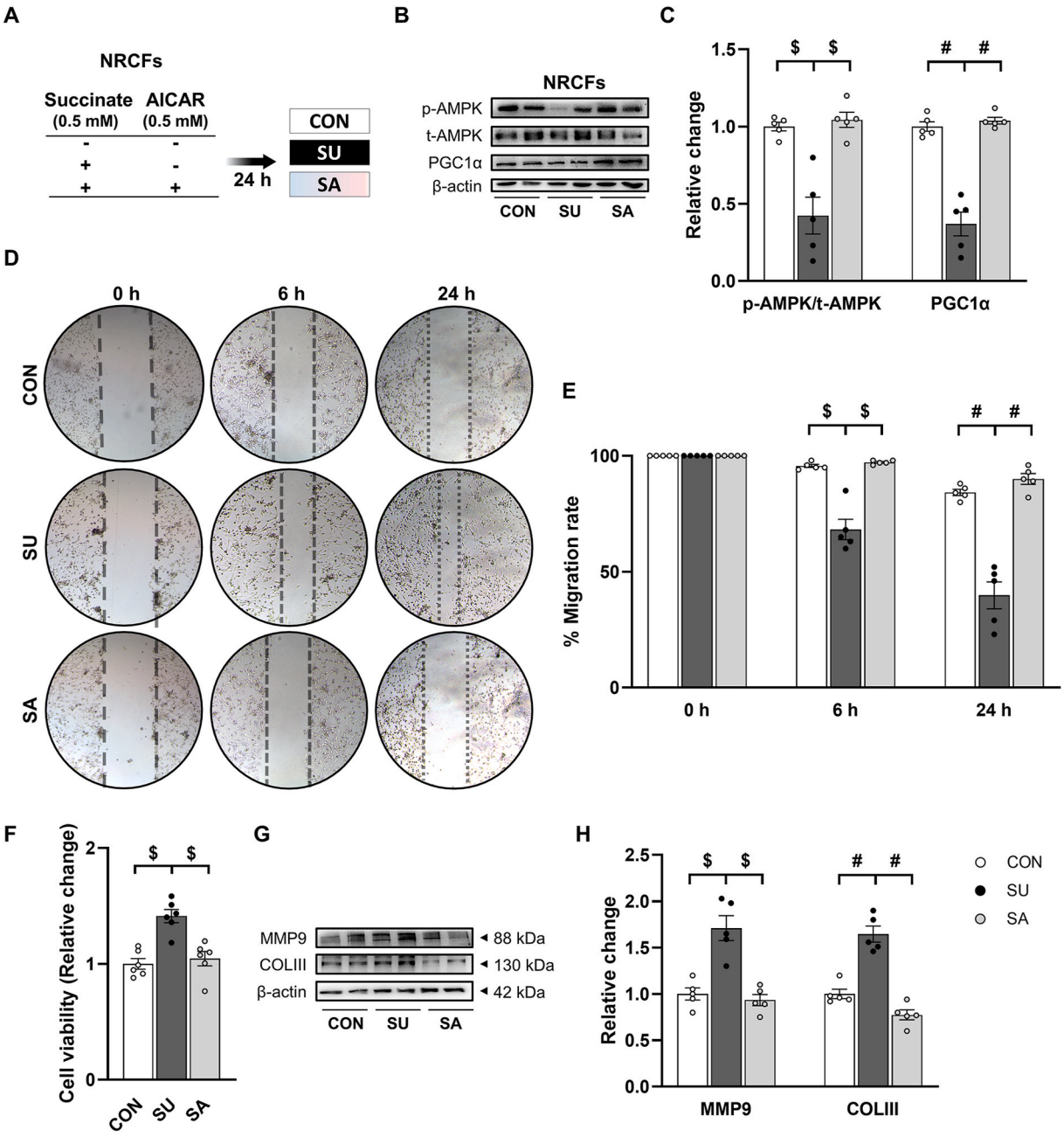

Fig. 9. AMPK activation via AICAR *attenuated succinate-induced fibrosis in NRCFs.* (A) Schematic representation of the cell experimental design. (B) Representative Western blot images and (C) quantification of AMPK and PGC1α signaling in isolated NRCFs treated with succinate and/or AICAR. (D–E) Cell migration assay of treated NRCFs. (F) Cell viability evaluated by Cell Counting Kit-8 in treated NRCFs. (G) Representative Western blot images and (H) quantification of fibrosis markers, including MMP9, COLI, and COLIII in treated NRCFs. SU, succinate; SA, succinate combined with AICAR. Data are shown as mean ± SEM. n = 5–6. $^{*}p < 0.05$, $^{**}p < 0.01$, $^{\$}p < 0.001$, $^{\#}p < 0.0001$ (Two-way ANOVA with Bonferroni *post-hoc* test).

cumulative mitochondrial impairments modify cardiomyocyte electrophysiological properties and promote abnormal substrate deposition, including fibrosis and collagen accumulation, ultimately predisposing the heart to AF [7] (Figs. 1–3).

Beyond its role in mitochondrial function, succinate also plays critical roles in other physiologically important processes, including innate immunity [37], paracrine or endocrine regulation [38], insulin biosynthesis/secretion [39], chromatin modifications (histones and DNA methylation) [13], and protein succinylation [40]. Specifically, succinate activates SUCNR1, a G-protein coupled receptor, leading to increased pro-inflammatory responses in macrophages [37] and promoting fibroblast proliferation and collagen synthesis in extra-atrial tissues such as the ventricle, liver, lung, and skin [41,42]. Furthermore, succinate can induce hypertension by stimulating the renal renin-angiotensin system [19] and disrupt metabolic balance through excessive atrial protein succinylation, potentially affecting the cellular structure and extracellular matrix [43]. These broad effects emphasize the intricate pathophysiology of succinate-induced AF and underscore the importance of further research to explore its potential role in regulating AF risk.

Therapy targeting succinate overload offers a promising alternative for managing AF. Supportively, modulation of succinate levels using dietary interventions [44], genetic modifications [45], chronic exercise [46], and medications such as metformin [47] have demonstrated potential metabolic benefits in addressing AF risk factors, including obesity and T2DM. In addition, its downstream target AMPK, a vital guardian of

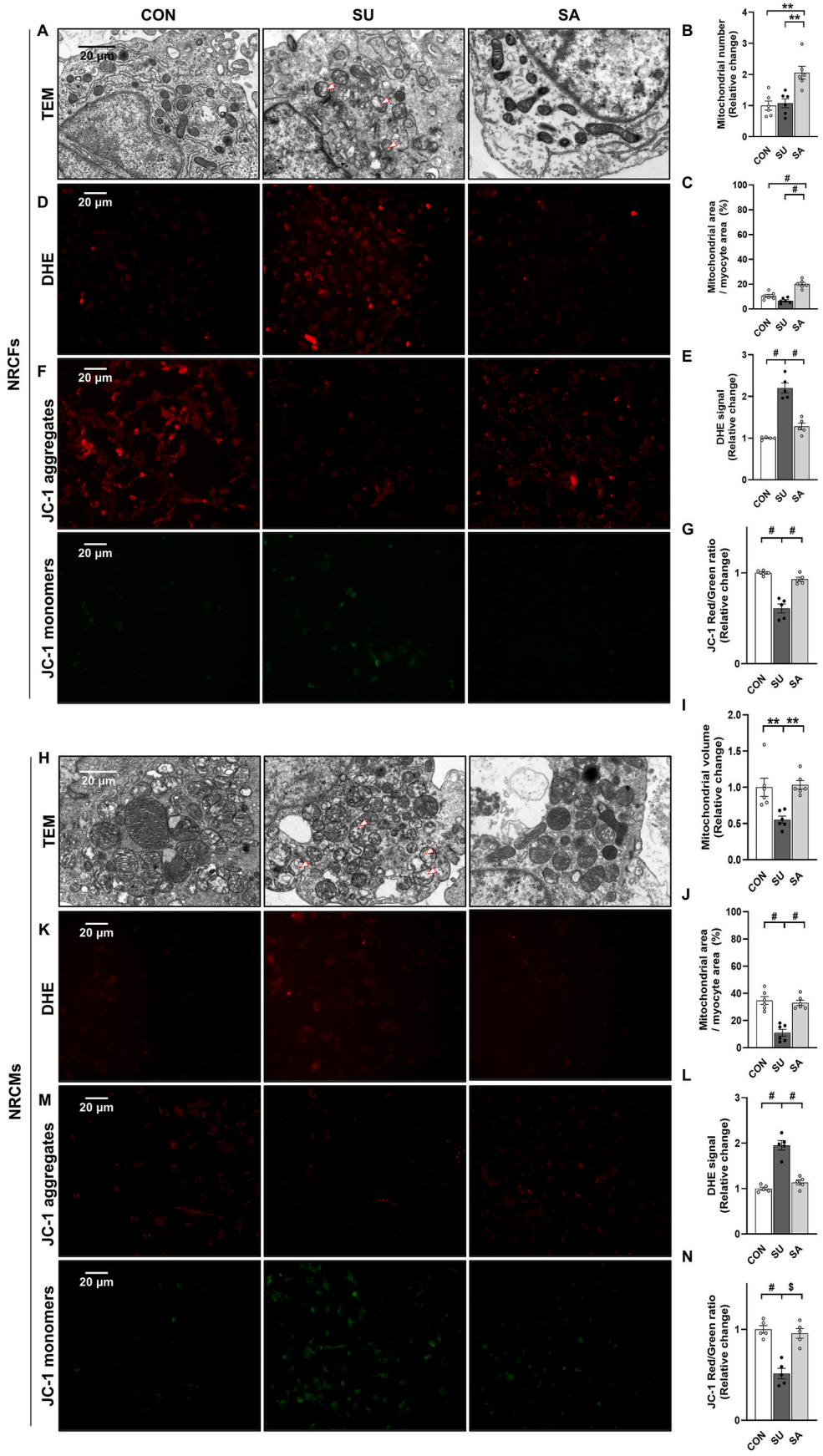

(caption on next page)

Fig. 10. AMPK activation restored succinate-induced mitochondrial dysfunction in NRCFs *and NRCMs.* (A) Representative longitudinal TEM images of mitochondrial morphology and quantification of (B) mitochondrial number and (C) mitochondrial volume density in isolated NRCFs treated with succinate and/or AICAR. Triangles indicate mitochondrial swelling. (D–E) Representative immunofluorescence staining of DHE and the analysis of oxidation products in treated NRCFs. (F–G) Fluorescent microscopic images of JC-1 staining and the analysis of red/green fluorescence ratio reflecting changes in the mitochondrial membrane potential (Δψm) in NRCFs. (H–N) The same experiments were performed in NRCMs as in NRCFs. SU, succinate; SA, succinate combined with AICAR. Data are shown as mean ± SEM. n = 6. $^{*}p < 0.05$, $^{**}p < 0.01$, $^{\$}p < 0.001$, $^{\#}p < 0.0001$ (Two-way ANOVA with Bonferroni *post-hoc* test).

metabolism and mitochondrial welfare [48], is envisaged as a potential therapeutic target for AF [49]. Our findings reveal that succinate inactivates atrial AMPK through SUCNR1 activation, while AMPK activation reduces circulating succinate levels and alleviates AF by preserving mitochondrial function (Figs. 6–10). Interestingly, prior research has reported that transient succinate accumulation can activate AMPK via the Ca^{2+}/p-CaMKK2 axis in prostate cancer cells [50]. This discrepancy may be explained by the different temporal dynamics of succinate accumulation. For example, atrial phosphorylated AMPK has been shown to increase adaptively in paroxysmal AF under metabolic stress but is markedly decreased in chronic AF [49]. In our model, prolonged succinate overload in atria resulted in decreased ATP levels and increased ROS, which failed to activate AMPK. Consequently, multiple AMPK-regulated pathways, including those involved in lipid metabolism, the TCA cycle, antioxidant defense, mitochondrial biogenesis, and mitochondrial dynamics, were suppressed (Fig. 5). These findings highlight the intricate interplay between succinate and AMPK signaling, emphasizing the need for further investigation into their mechanistic crosstalk and implications for AF pathogenesis and therapy.

Interestingly, recent advances have identified the health-promoting effects of succinate in certain physiological and pathological settings. For example, enhanced succinate dehydrogenation in the heart [46] and muscle [51] following chronic physical exercise improves cardiometabolic fitness by mitochondrial remodeling. Additionally, succinate released in response to exercise supports muscle adaptation to endurance by promoting glycolysis and amino acid catabolism [51]. Gut microbiota-derived succinate has been shown to mitigate systemic insulin resistance and conditions like dyslipidemia and nonalcoholic fatty liver disease [52] through the activation of intestinal gluconeogenesis [26] and thermogenesis in brown adipose tissue [25], particularly in obesity. However, most of these studies involve short-term treatments and maintain succinate levels within the physiological range. Our unpublished work showed that prolonged succinate supplement deteriorated glucose and insulin homeostasis in lean mice (2 % in drinking water for 7 weeks), which is consistent with our results demonstrating that 7-week succinate treatment predisposes mice to AF by impairing mitochondrial function. This effect may be due to the fact that atrial tissue relies heavily on fatty acid oxidation (FAO) and is less adaptable to a shift towards glycolysis in long-term substrate metabolism, in contrast to other tissues such as the intestine, adipose, liver, and muscle, which have more metabolic flexibility [3]. Thus, while succinate may have beneficial effects under certain conditions, its prolonged overload can have detrimental consequences, particularly in tissues with limited metabolic adaptability like the atria.

Despite recent progress, a few questions remain to be answered. First, while our data establish that succinate overload predisposes healthy mice to AF and mediates obesity- and T2DM-associated AF, succinate serves multiple intracellular and systemic functions. Its role as either a contributor to or a protector against AF in diverse etiologies, such as aging and hypertension, remains inconclusive and warrants further investigation. Second, although succinate shows promise as a circulating biochemical marker for AF [21], its clinical utility across different AF populations remains undetermined. Future prospective studies with larger, stratified cohorts are needed to validate its diagnostic and prognostic value. Third, the therapeutic strategies for regulating succinate levels are still largely undefined. Succinate can be physiologically released by the microbiota, diet, and dying epithelial cells, or pathologically produced by exercised skeletal muscle [51], ischemic heart [34], and damaged liver [53]. The unclear origins of succinate and the identification of optimal therapeutic targets require further clarification in diverse AF populations. Additionally, since SDH activity is influenced by the intensity and duration of physical training, succinate modulation may depend significantly on tailored therapeutic approaches [54]. Consequently, the manipulation of succinate metabolism for AF management must be personalized, supported by further functional and mechanistic studies.

5. Conclusion

We show the first direct evidence linking succinic acid overload to an increased AF risk, revealing its underlying mechanism of impairing AMPK signaling and mitochondrial function. Notably, we demonstrate that AMPK activation can effectively counteract succinate-induced AF by restoring mitochondrial integrity and function. These findings highlight succinate overload as a novel mitochondrial pathomechanism contributing to AF and underscore its potential as a valuable biomarker for AF risk assessment and therapeutic targeting.

CRediT authorship contribution statement

Yudi Zhang: Writing – original draft, Validation, Methodology, Investigation, Formal analysis, Data curation, Conceptualization. **Haoyu Gong:** Writing – review & editing, Validation, Methodology, Investigation, Formal analysis. **Lingyan Jin:** Methodology, Investigation, Data curation. **Peng Liu:** Software, Project administration. **Jiali Fan:** Visualization, Methodology. **Xinghua Qin:** Writing – review & editing, Supervision, Project administration, Funding acquisition. **Qiangsun Zheng:** Supervision, Resources, Funding acquisition, Conceptualization.

Ethical approval

Approved by the Institutional Animal Care and Use Committee of XJTU (Grant Number 2021-932). Not a clinical study.

Funding

National Natural Science Foundation of China: 31871172, 82270335, 32371164; Key Research and Development Project of Shaanxi Province: 2023-YBSF-600, 2021SF-132.

Declaration of competing interest

The authors declare that they have no known competing financial interests or personal relationships that could have appeared to influence the work reported in this paper.

Acknowledgments

We thank the technical assistance of Professor Liping Yuan, Associate Professor Changyang Xing, and Master's student Wei Hu (Tangdu Hospital).

Appendix A. Supplementary data

Supplementary data to this article can be found online at https://doi.org/10.1016/j.redox.2025.103576.

Data availability

Data will be made available on request.

References

[1] G. Lippi, F. Sanchis-Gomar, G. Cervellin, Global epidemiology of atrial fibrillation: an increasing epidemic and public health challenge, Int. J. Stroke 16 (2021) 217–221, https://doi.org/10.1177/1747493019897870.

[2] B.J.J.M. Brundel, X. Ai, M.T. Hills, M.F. Kuipers, G.Y.H. Lip, N.M.S. De Groot, Atrial fibrillation, Nat. Rev. Dis. Primers 8 (2022) 21, https://doi.org/10.1038/s41572-022-00347-9.

[3] X. Qin, Y. Zhang, Q. Zheng, Metabolic inflexibility as a pathogenic basis for atrial fibrillation, Int. J. Mol. Sci. 23 (2022) 8291, https://doi.org/10.3390/ijms23158291.

[4] X. Qin, L. Jin, H. Gong, Q. Zheng, Electro-metabolic coupling in atrial fibrillation: a deeper understanding of the metabolic driver, Biomed. Pharmacother. 180 (2024) 117536, https://doi.org/10.1016/j.biopha.2024.117536.

[5] D. Opacic, K.A. Van Bragt, H.M. Nasrallah, U. Schotten, S. Verheule, Atrial metabolism and tissue perfusion as determinants of electrical and structural remodelling in atrial fibrillation, Cardiovasc. Res. 109 (2016) 527–541, https://doi.org/10.1093/cvr/cvw007.

[6] E.J. Griffiths, Mitochondria and heart disease, Adv. Exp. Med. Biol. 942 (2012) 249–267, https://doi.org/10.1007/978-94-007-2869-1_11.

[7] P. Muszyński, T.A. Bonda, Mitochondrial dysfunction in atrial fibrillation—mechanisms and pharmacological interventions, J. Clin. Med. 10 (2021) 2385, https://doi.org/10.3390/jcm10112385.

[8] S.M. Brown, N.K. Larsen, F.G. Thankam, D.K. Agrawal, Regulatory role of cardiomyocyte metabolism via AMPK activation in modulating atrial structural, contractile, and electrical properties following atrial fibrillation, Can. J. Physiol. Pharmacol. 99 (2021) 36–41, https://doi.org/10.1139/cjpp-2020-0313.

[9] X. Qin, Y. Fu, J. Fan, B. Liu, P. Liu, Y. Zhang, T. Jiang, Q. Zheng, Melatonin increases susceptibility to atrial fibrillation in obesity via Akt signaling impairment in response to lipid overload, J. Pineal Res. 74 (2023) e12851, https://doi.org/10.1111/jpi.12851.

[10] L. Tretter, A. Patocs, C. Chinopoulos, Succinate, an intermediate in metabolism, signal transduction, ROS, hypoxia, and tumorigenesis, Biochim. Biophys. Acta BBA - Bioenerg. 1857 (2016) 1086–1101, https://doi.org/10.1016/j.bbabio.2016.03.012.

[11] I.N. Watt, M.G. Montgomery, M.J. Runswick, A.G.W. Leslie, J.E. Walker, Bioenergetic cost of making an adenosine triphosphate molecule in animal mitochondria, Proc. Natl. Acad. Sci. USA 107 (2010) 16823–16827, https://doi.org/10.1073/pnas.1011099107.

[12] E.T. Chouchani, V.R. Pell, E. Gaude, D. Aksentijević, S.Y. Sundier, E.L. Robb, A. Logan, S.M. Nadtochiy, E.N.J. Ord, A.C. Smith, F. Eyassu, R. Shirley, C.-H. Hu, A.J. Dare, A.M. James, S. Rogatti, R.C. Hartley, S. Eaton, A.S.H. Costa, P. S. Brookes, S.M. Davidson, M.R. Duchen, K. Saeb-Parsy, M.J. Shattock, A. J. Robinson, L.M. Work, C. Frezza, T. Krieg, M.P. Murphy, Ischaemic accumulation of succinate controls reperfusion injury through mitochondrial ROS, Nature 515 (2014) 431–435, https://doi.org/10.1038/nature13909.

[13] A. Salminen, K. Kaarniranta, M. Hiltunen, A. Kauppinen, Krebs cycle dysfunction shapes epigenetic landscape of chromatin: novel insights into mitochondrial regulation of aging process, Cell. Signal. 26 (2014) 1598–1603, https://doi.org/10.1016/j.cellsig.2014.03.030.

[14] E. Mills, L.A.J. O'Neill, Succinate: a metabolic signal in inflammation, Trends Cell Biol. 24 (2014) 313–320, https://doi.org/10.1016/j.tcb.2013.11.008.

[15] H.A. Prag, A.V. Gruszczyk, M.M. Huang, T.E. Beach, T. Young, L. Tronci, E. Nikitopoulou, J.F. Mulvey, R. Ascione, A. Hadjihambi, M.J. Shattock, L. Pellerin, K. Saeb-Parsy, C. Frezza, A.M. James, T. Krieg, M.P. Murphy, D. Aksentijević, Mechanism of succinate efflux upon reperfusion of the ischaemic heart, Cardiovasc. Res. 117 (2021) 1188–1201, https://doi.org/10.1093/cvr/cvaa148.

[16] G. Caluori, F. Vaillant, E. Abell, F. Ichou, V. Loyer, A. Haeberlin, S. Ploux, H. A. Mahamat, R. Dubois, B. Guillot, P. Diolez, V. Meillet, S. Hatem, P. Krisai, T. Kamakura, M. Hocini, O. Bernus, P. Santos, P. Jais, P. Pasdois, B-po02-032 succinate accumulation in atrial cardiomyocytes increases mitochondrial reverse electron flux, oxidative stress, and might participate to af stabilization in the sheep, Heart Rhythm 18 (2021) S107–S108.

[17] M. Gawałko, T.A. Agbaedeng, A. Saljic, D.N. Müller, N. Wilck, R. Schnabel, J. Penders, M. Rienstra, I. Van Gelder, T. Jespersen, U. Schotten, H.J.G.M. Crijns, J. M. Kalman, P. Sanders, S. Nattel, D. Dobrev, D. Linz, Gut microbiota, dysbiosis and atrial fibrillation. Arrhythmogenic mechanisms and potential clinical implications, Cardiovasc. Res. 118 (2022) 2415–2427, https://doi.org/10.1093/cvr/cvab292.

[18] C. Serena, V. Ceperuelo-Mallafré, N. Keiran, M.I. Queipo-Ortuño, R. Bernal, R. Gomez-Huelgas, M. Urpi-Sarda, M. Sabater, V. Pérez-Brocal, C. Andrés-Lacueva, A. Moya, F.J. Tinahones, J.M. Fernández-Real, J. Vendrell, S. Fernández-Veledo, Elevated circulating levels of succinate in human obesity are linked to specific gut microbiota, ISME J. 12 (2018) 1642–1657, https://doi.org/10.1038/s41396-018-0068-2.

[19] Circulating succinate is elevated in rodent models of hypertension and metabolic disease, Am. J. Hypertens. 20 (2007) 1209–1215, https://doi.org/10.1016/j.amjhyper.2007.05.010.

[20] F.J. Osuna-Prieto, B. Martinez-Tellez, L. Ortiz-Alvarez, X. Di, L. Jurado-Fasoli, H. Xu, V. Ceperuelo-Mallafré, C. Núñez-Roa, I. Kohler, A. Segura-Carretero, J. V. García-Lario, A. Gil, C.M. Aguilera, J.M. Llamas-Elvira, P.C.N. Rensen, J. Vendrell, J.R. Ruiz, S. Fernández-Veledo, Elevated plasma succinate levels are linked to higher cardiovascular disease risk factors in young adults, Cardiovasc. Diabetol. 20 (2021) 151, https://doi.org/10.1186/s12933-021-01333-3.

[21] M. Bulló, C. Papandreou, J. García-Gavilán, M. Ruiz-Canela, J. Li, M. Guasch-Ferré, E. Toledo, C. Clish, D. Corella, R. Estruch, E. Ros, M. Fitó, C.-H. Lee, K. Pierce, C. Razquin, F. Arós, L. Serra-Majem, L. Liang, M.A. Martínez-González, F.B. Hu, J. Salas-Salvadó, Tricarboxylic acid cycle related-metabolites and risk of atrial fibrillation and heart failure, Metabolism 125 (2021) 154915, https://doi.org/10.1016/j.metabol.2021.154915.

[22] S.E. Nelson, Z. Ament, Z. Wolcott, R.E. Gerszten, W.T. Kimberly, Succinate links atrial dysfunction and cardioembolic stroke, Neurology 92 (2019), https://doi.org/10.1212/WNL.0000000000006957.

[23] S.Y. Park, C.T. Le, K.Y. Sung, D.H. Choi, E.-H. Cho, Succinate induces hepatic fibrogenesis by promoting activation, proliferation, and migration, and inhibiting apoptosis of hepatic stellate cells, Biochem. Biophys. Res. Commun. 496 (2018) 673–678, https://doi.org/10.1016/j.bbrc.2018.01.106.

[24] Y. Wang, X. Zhang, H. Yao, X. Chen, L. Shang, P. Li, X. Cui, J. Zeng, Peroxisome-generated succinate induces lipid accumulation and oxidative stress in the kidneys of diabetic mice, J. Biol. Chem. 298 (2022) 101660, https://doi.org/10.1016/j.jbc.2022.101660.

[25] E.L. Mills, K.A. Pierce, M.P. Jedrychowski, R. Garrity, S. Winther, S. Vidoni, T. Yoneshiro, J.B. Spinelli, G.Z. Lu, L. Kazak, A.S. Banks, M.C. Haigis, S. Kajimura, M.P. Murphy, S.P. Gygi, C.B. Clish, E.T. Chouchani, Accumulation of succinate controls activation of adipose tissue thermogenesis, Nature 560 (2018) 102–106, https://doi.org/10.1038/s41586-018-0353-2.

[26] F. De Vadder, P. Kovatcheva-Datchary, C. Zitoun, A. Duchampt, F. Bäckhed, G. Mithieux, Microbiota-produced succinate improves glucose homeostasis via intestinal gluconeogenesis, Cell Metab. 24 (2016) 151–157, https://doi.org/10.1016/j.cmet.2016.06.013.

[27] Y. Zhang, F. Gao, H. Gong, Y. Fu, B. Liu, X. Qin, Q. Zheng, Intermittent fasting attenuates obesity-related atrial fibrillation via SIRT3-mediated insulin resistance mitigation, Biochim. Biophys. Acta BBA - Mol. Basis Dis. 1869 (2023) 166638, https://doi.org/10.1016/j.bbadis.2023.166638.

[28] C. Ozcan, Z. Li, G. Kim, V. Jeevanandam, N. Uriel, Molecular mechanism of the association between atrial fibrillation and heart failure includes energy metabolic dysregulation due to mitochondrial dysfunction, J. Card. Fail. 25 (2019) 911–920, https://doi.org/10.1016/j.cardfail.2019.08.005.

[29] W. Xie, G. Santulli, S.R. Reiken, Q. Yuan, B.W. Osborne, B.-X. Chen, A.R. Marks, Mitochondrial oxidative stress promotes atrial fibrillation, Sci. Rep. 5 (2015) 11427, https://doi.org/10.1038/srep11427.

[30] D. Dobrev, S. Nattel, Calcium handling abnormalities in atrial fibrillation as a target for innovative therapeutics, J. Cardiovasc. Pharmacol. 52 (2008) 293–299, https://doi.org/10.1097/FJC.0b013e318171924d.

[31] W.G. Kaelin, P.J. Ratcliffe, Oxygen sensing by metazoans: the central role of the HIF hydroxylase pathway, Mol. Cell 30 (2008) 393–402, https://doi.org/10.1016/j.molcel.2008.04.009.

[32] V.R. Pell, E.T. Chouchani, C. Frezza, M.P. Murphy, T. Krieg, Succinate metabolism: a new therapeutic target for myocardial reperfusion injury, Cardiovasc. Res. 111 (2016) 134–141, https://doi.org/10.1093/cvr/cvw100.

[33] Y.-T. Lu, L.-Z. Li, Y.-L. Yang, X. Yin, Q. Liu, L. Zhang, K. Liu, B. Liu, J. Li, L.-W. Qi, Succinate induces aberrant mitochondrial fission in cardiomyocytes through GPR91 signaling, Cell Death Dis. 9 (2018) 672, https://doi.org/10.1038/s41419-018-0708-5.

[34] T.N. Andrienko, P. Pasdois, G.C. Pereira, M.J. Ovens, A.P. Halestrap, The role of succinate and ROS in reperfusion injury – a critical appraisal, J. Mol. Cell. Cardiol. 110 (2017) 1–14, https://doi.org/10.1016/j.yjmcc.2017.06.016.

[35] T. Bourgeron, P. Rustin, D. Chretien, M. Birch-Machin, M. Bourgeois, E. Viegas-Péquignot, A. Munnich, A. Rötig, Mutation of a nuclear succinate dehydrogenase gene results in mitochondrial respiratory chain deficiency, Nat. Genet. 11 (1995) 144–149, https://doi.org/10.1038/ng1095-144.

[36] C.J. Aguiar, V.L. Andrade, E.R.M. Gomes, M.N.M. Alves, M.S. Ladeira, A.C. N. Pinheiro, D.A. Gomes, A.P. Almeida, A.M. Goes, R.R. Resende, S. Guatimosim, M.F. Leite, Succinate modulates Ca2+ transient and cardiomyocyte viability through PKA-dependent pathway, Cell Calcium 47 (2010) 37–46, https://doi.org/10.1016/j.ceca.2009.11.003.

[37] G.M. Tannahill, A.M. Curtis, J. Adamik, E.M. Palsson-McDermott, A.F. McGettrick, G. Goel, C. Frezza, N.J. Bernard, B. Kelly, N.H. Foley, L. Zheng, A. Gardet, Z. Tong, S.S. Jany, S.C. Corr, M. Haneklaus, B.E. Caffrey, K. Pierce, S. Walmsley, F. C. Beasley, E. Cummins, V. Nizet, M. Whyte, C.T. Taylor, H. Lin, S.L. Masters, E. Gottlieb, V.P. Kelly, C. Clish, P.E. Auron, R.J. Xavier, L.A.J. O'Neill, Succinate is an inflammatory signal that induces IL-1β through HIF-1α, Nature 496 (2013) 238–242, https://doi.org/10.1038/nature11986.

[38] M.P. Murphy, E.T. Chouchani, Why succinate? Physiological regulation by a mitochondrial coenzyme Q sentinel, Nat. Chem. Biol. 18 (2022) 461–469, https://doi.org/10.1038/s41589-022-01004-8.

[39] V. Attali, M. Parnes, Y. Ariav, E. Cerasi, N. Kaiser, G. Leibowitz, Regulation of insulin secretion and proinsulin biosynthesis by succinate, Endocrinology 147 (2006) 5110–5118, https://doi.org/10.1210/en.2006-0496.

[40] X. Hou, Y. Chen, X. Li, X. Gu, W. Dong, J. Shi, S. Ji, Protein succinylation: regulating metabolism and beyond, Front. Nutr. 11 (2024) 1336057, https://doi.org/10.3389/fnut.2024.1336057.
[41] A.C. Ariza, P.M.T. Deen, J.H. Robben, The succinate receptor as a novel therapeutic target for oxidative and metabolic stress-related conditions, Front. Endocrinol. 3 (2012), https://doi.org/10.3389/fendo.2012.00022.
[42] J. Henderson, S. O'Reilly, The emerging role of metabolism in fibrosis, Trends Endocrinol, Metabolism 32 (2021) 639–653, https://doi.org/10.1016/j.tem.2021.05.003.
[43] F. Bai, T. Tu, F. Qin, Y. Ma, N. Liu, Y. Liu, X. Liao, S. Zhou, Q. Liu, Quantitative proteomics of changes in succinylated proteins expression profiling in left appendages tissue from valvular heart disease patients with atrial fibrillation, Clin. Chim. Acta 495 (2019) 345–354, https://doi.org/10.1016/j.cca.2019.05.002.
[44] S. Fernández-Veledo, J. Vendrell, Gut microbiota-derived succinate: friend or foe in human metabolic diseases? Rev. Endocr. Metab. Disord. 20 (2019) 439–447, https://doi.org/10.1007/s11154-019-09513-z.
[45] J. Lu, J. Li, H. Gao, D. Zhou, H. Xu, Y. Cong, W. Zhang, F. Xin, M. Jiang, Recent progress on bio-succinic acid production from lignocellulosic biomass, World J. Microbiol. Biotechnol. 37 (2021) 16, https://doi.org/10.1007/s11274-020-02979-z.
[46] M. Balietti, P. Fattoretti, M. Skalicky, A. Viidik, B. Giorgetti, Y. Grossi, C. Bertoni-Freddari, The effect of chronic physical exercise on succinic dehydrogenase activity in the heart muscle of old rats, Biogerontology 6 (2005) 95–100, https://doi.org/10.1007/s10522-005-3463-9.
[47] Y. Tanaka, A. Konishi, H. Obinata, M. Tsuneoka, Metformin activates KDM2A to reduce rRNA transcription and cell proliferation by dual regulation of AMPK activity and intracellular succinate level, Sci. Rep. 9 (2019) 18694, https://doi.org/10.1038/s41598-019-55075-0.
[48] S. Herzig, R.J. Shaw, AMPK: guardian of metabolism and mitochondrial homeostasis, Nat. Rev. Mol. Cell Biol. 19 (2018) 121–135, https://doi.org/10.1038/nrm.2017.95.
[49] G.E. Kim, L.H. Young, AMPK and the atrial response to metabolic inhibition, J. Am. Coll. Cardiol. 66 (2015) 59–61, https://doi.org/10.1016/j.jacc.2015.04.054.
[50] N. Saxena, E. Beraldi, L. Fazli, S.P. Somasekharan, H. Adomat, F. Zhang, C. Molokwu, A. Gleave, L. Nappi, K. Nguyen, P. Brar, N. Nikesitch, Y. Wang, C. Collins, P.H. Sorensen, M. Gleave, Androgen receptor (AR) antagonism triggers acute succinate-mediated adaptive responses to reactivate AR signaling, EMBO Mol. Med. 13 (2021) e13427, https://doi.org/10.15252/emmm.202013427.
[51] A. Reddy, L.H.M. Bozi, O.K. Yaghi, E.L. Mills, H. Xiao, H.E. Nicholson, M. Paschini, J.A. Paulo, R. Garrity, D. Laznik-Bogoslavski, J.C.B. Ferreira, C.S. Carl, K. A. Sjøberg, J.F.P. Wojtaszewski, J.F. Jeppesen, B. Kiens, S.P. Gygi, E.A. Richter, D. Mathis, E.T. Chouchani, pH-gated succinate secretion regulates muscle remodeling in response to exercise, Cell 183 (2020) 62–75.e17, https://doi.org/10.1016/j.cell.2020.08.039.
[52] K. Wang, M. Liao, N. Zhou, L. Bao, K. Ma, Z. Zheng, Y. Wang, C. Liu, W. Wang, J. Wang, S.-J. Liu, H. Liu, Parabacteroides distasonis alleviates obesity and metabolic dysfunctions via production of succinate and secondary bile acids, Cell Rep. 26 (2019) 222–235.e5, https://doi.org/10.1016/j.celrep.2018.12.028.
[53] P.R.A.V. Correa, E.A. Kruglov, M. Thompson, M.F. Leite, J.A. Dranoff, M. H. Nathanson, Succinate is a paracrine signal for liver damage, J. Hepatol. 47 (2007) 262–269, https://doi.org/10.1016/j.jhep.2007.03.016.
[54] G.L. Dohm, G.R. Beecher, T.P. Stephenson, M. Womack, Adaptations to endurance training at three intensities of exercise, J. Appl. Physiol. 42 (1977) 753–757, https://doi.org/10.1152/jappl.1977.42.5.753.